Strain transfer and partitioning between the Panamint Valley, Searles Valley, and Ash Hill fault zones, California

J. Douglas Walker
Department of Geology, University of Kansas, Lawrence, Kansas 66045, USA

Eric Kirby
Department of Geosciences, Pennsylvania State University, University Park, Pennsylvania 16802, USA

Joseph E. Andrew
Department of Geology, Youngstown State University, Youngstown, Ohio 44555, USA

ABSTRACT

We report new geologic and geomorphic observations that bear on the interpretation of connectivity and strain transfer among the Panamint Valley, Searles Valley, and Ash Hill fault zones, southern Walker Lane belt of California. Although these faults partition strain regionally onto dominantly normal and strike-slip structures, strain transfer occurs in a complex way not typical of linked strike-slip and extensional faults. The Searles Valley fault (W-directed normal fault) transfers slip onto the Panamint Valley zone, which changes from dominantly NNW-trending dextral strike-slip to more normal motion where they join. The Ash Hill fault (mostly right-lateral strike slip) transfers strain into the northern continuation of the Searles Valley zone, via a complex array of hanging-wall normal and strike-slip faults. These complex interactions, based on the age of structurally offset markers, appear to be stable over ~10^5 years.

Keywords: strain transfer, transtension, Panamint Valley, Searles Valley, faulting.

INTRODUCTION AND TECTONIC SETTING

Areas undergoing active deformation are typically viewed at two levels of observation and analysis. In the larger view, the regional maximum extension-and-contraction (for strain) or tension-and-compression (for stress) directions provide major boundary conditions on the nature of deformation. In a more detailed view, slip and interactions of faults (as well as other structures) or the stress distribution are of greater interest. The link between these scales is that the regional pattern must be accommodated by motions on individual faults and other structures. In this paper, we address fault slip at the more detailed level in an area experiencing transtensional deformation. We will describe how slip varies between different individual fault zones (defining partitioning of slip or strain on local structures), and how the slip changes or transfers in areas where fault zones of different character interact. In general, we consider strain transfer to reflect slip and/or geometry change along the strike direction of a fault zone into an area of interaction with another structure. In contrast, strain partitioning describes how fault zones divide slip onto individual structures across a belt of deformation (e.g., across strike).

A detailed understanding of transtensional deformation requires knowing how strain partitions regionally between subjacent fault strands and how it transfers locally between structures. Interpretation of geodetic velocity fields, earthquake rupture and propagation, and the consequent magnitude of seismic events all depend critically on the nature of fault linkage. Although a significant body of work has focused on the growth and linkage of normal fault systems (e.g., Dawers et al., 1993; Cowie and Scholz, 1992), fewer studies have looked at the manner of strain transfer in transtensional settings (e.g., Oldow, 1992; Reheis and Dixon, 1996), where the direction of maximum finite elongation is oblique to the boundaries of the zone of deformation (e.g., Dewey et al., 1998). This is an especially interesting setting because both dominantly transcurrent and normal faults are present in close association.

Within transtensional shear zones, fault displacement may be transferred from one fault zone to another. Strain transfer in transtensional zones is commonly accomplished by normal slip on faults linked to subjacent strike-slip faults (e.g., Burchfiel and Stewart, 1966; Reheis and Dixon, 1996), but other, more complex interactions are common (e.g., Faulds and Varga, 1998; Manighetti et al., 2001). Strain partitioning is best illustrated by coordinated regional fault arrays that variously display strike slip or normal slip on individual structures. Caskey et al. (1996) presented a compelling case for the nature of strain transfer and partitioning for the Dixie Valley–Fairview Peak earthquake sequence of 1954. These authors documented dip-slip and strike-slip faulting coordinated on adjacent, and in some cases, related structures in a single faulting event. In addition, when considered along with the Rainbow Mountain and Stillwater earthquakes (same year as Dixie Valley–Fairview Peak), these faults record important strain partitioning. This example clearly shows the complex way slip can be divided on faults at the time scale of a single earthquake cycle.

The aim of this paper is to examine strain transfer and partitioning at somewhat longer time scales than earthquakes or yearly geodetic measurements for the Searles Valley–Panamint Valley area of the eastern California shear zone–southern Walker Lane belt (Fig. 1). Although this region experienced severe extensional deformation during Miocene to Pliocene time, the present-day strain field is characterized by transcurrent right-lateral shear (e.g., Miller et al., 2001) that is accom-
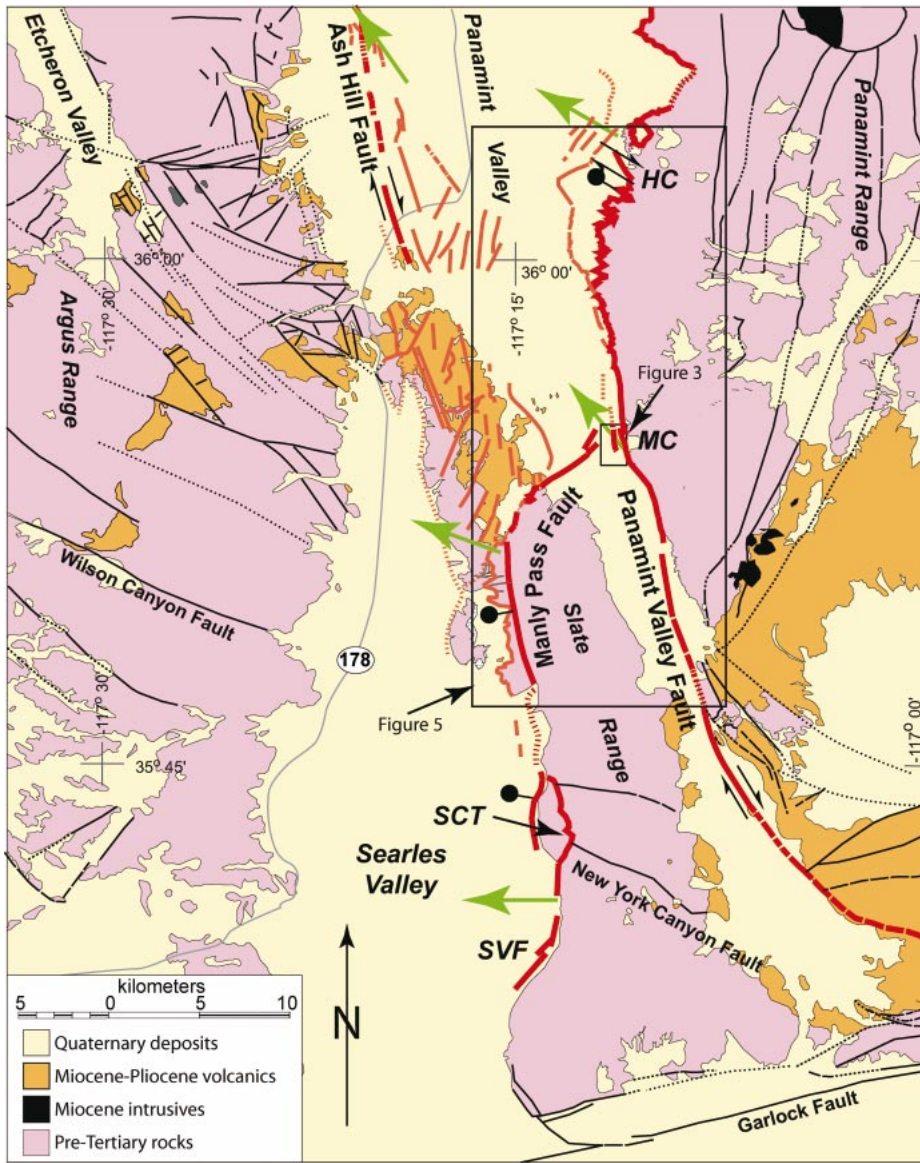
Figure 1. Location map for the Searles Valley–Panamint Valley study area. Active faults considered in our analysis are shown in red, and main bounding structures (Ash Hill, Manly Pass, Searles Valley, and Panamint Valley fault zones) are shown as bold lines; other regional faults are shown as bold black lines. Fault systems are somewhat simplified. Green arrows point in direction of slip for the various fault zones (as described in text); vector for Ash Hill system is actually determined for an area ~30 km north of the figure. The Garlock fault is on the southern boundary of the area, and Death Valley is located to the east of the Panamint Range. The locations of Figures 3 and 5 are indicated by boxes. HC—Hall Canyon; MC—Manly canyon; SCT—Sand Canyon thrust; SVF— Searles Valley fault. Sand Canyon is located where the arrow from SCT crosses the range front. Base map modified from Walker et al. (2002).

modated on several major oblique-normal faults in the Death, Panamint, Searles, and Indian Wells valleys (Fig. 1). The onset of this transition occurred in late Miocene to Pleistocene time (Wernicke et al., 1988; Bellier and Zoback, 1995; Wernicke and Snow, 1998; Snow and Wernicke, 2000; Monastero et al.,

2002). Active faulting in this area is well documented by seismic (e.g., Wallace, 1984) and global-positioning-system (GPS) studies (Dixon et al., 1995, 2000), as well as by geologic investigations (Burchfiel et al., 1987; Zhang et al., 1990; Klinger and Piety, 2001; Andrew, 2002). The manner in which these fault sys-

tems interact has important implications for the distribution of strain across the region and for the interpretation of geodetic velocity fields (e.g., McClusky et al., 2001).

We consider the nature of deformation on structures that record activity over the past ~10–100 k.y. By focusing on this time interval, we are able to utilize geomorphic markers (primarily alluvial fan surfaces and related channels) to examine the manner in which displacement varies along strike of the fault systems. Because these markers integrate displacement over multiple earthquake cycles, and are not subject to the vagaries of a single rupture event (yet are younger than the life span of the fault systems), offsets derived from geomorphic observations can provide insight into the temporal evolution of fault displacement. Below, we describe fault displacement in the Panamint and Searles valleys, reconstruct fault slip from displaced geomorphic markers, and integrate these observations into a kinematic model for transtensional deformation in the region.

Geometry and Slip on Faults

The primary structures in the region are the Panamint Valley fault zone, the Searles Valley–Manly Pass fault system, and the Ash Hill fault (Fig. 1). This discussion centers on the nature of fault displacement; although we utilize existing temporal constraints on recent motion, we recognize that such data are sparse. Rather than focus on slip rates, we aim to establish the direction of slip and clarify the nature of fault interactions.

Searles Valley and Manly Pass Fault Zones

The Searles Valley and Manly Pass faults form the main structures along the western side of the Slate Range and across the northern Slate Range (Fig. 1), respectively. The active trace of the Searles Valley fault is marked by a series of scarps developed in Late Pleistocene–Holocene alluvial fans along the eastern margin of Searles Valley (Smith et al., 1968; Benson et al., 1990). South of Sand Canyon (at the arrow from SCT on Fig. 1), the scarps form a graben in alluvial fan deposits with a moderately well developed pavement. Stratigraphic observations indicate that alluvial fan gravel overlies carbonate-cemented beach gravel along most of the range front (Numelin and Kirby, 2004). These fans are overlapped along their distal margins by distinct shoreline features, including wave-cut platforms, tufa mounds, and beach deposits.

These stratigraphic relations are consistent with the chronology of similar beach deposits elsewhere in Searles Valley (Benson et al., 1990; Lin et al., 1998). We interpret the shoreline features to be associated with the last highstand of Searles Lake, and the beach deposits to be associated with the next older lake highstand. This suggests that alluvial fan gravels date to between 16 and 25 ka and 10–12 ka (Smith and Street-Perrott, 1984; Benson et al., 1990). Field relations indicate that scarps bounding the graben sole into a low-angle normal fault that forms the western margin of the Slate Range (Fig. 1). Thus, scarp formation is interpreted to reflect slip on the normal fault zone within the past 25–10 ka. Motion on this zone appears to be primarily dip-slip (with the horizontal component of slip trending ~270°); channels and debris-flow levees are not offset laterally by any significant amount across the graben and the fault trace is very sinuous as followed across topography (Numelin and Kirby, 2004).

The low-angle normal fault is continuous northward with the Sand Canyon "thrust" mapped by Smith et al. (1968). This fault is marked by the same character of gouge as observed along the low-angle normal fault, but is contained within bedrock of the Slate Range. Although these authors interpreted this structure as a thrust fault, it is clear that it accommodates some of the normal motion of the range-bounding fault (see also the discussion of Cichanski, 2000). Active normal faulting also continues north along the range front, west of the Sand Canyon fault. Prominent scarps displace alluvial fans that postdate the Searles Lake shorelines discussed above. Although the degree to which displacement is accommodated on these two structures is uncertain, the western set of scarps becomes less distinct and eventually dies out to the north along the range front (Fig. 1). These relations suggest that significant displacement passes up into the Slate Range along the Sand Canyon fault.

The Searles Valley fault zone continues northward to the Manly Pass normal fault zone in the northern Slate Range. The Manly Pass zone consists of the basal Manly Pass fault, a west-dipping normal fault, and a complexly deformed hanging wall containing numerous normal, strike-slip, and oblique-slip faults (Smith et al., 1968; Moore, 1976; Andrew and Walker, 2002). Footwall rocks consist of Mesozoic plutonic rocks containing local pendants of Paleozoic strata; to the east, these rocks are overlain nonconformably by Miocene volcanic and sedimentary rocks. The hanging wall consists of similar rocks as well
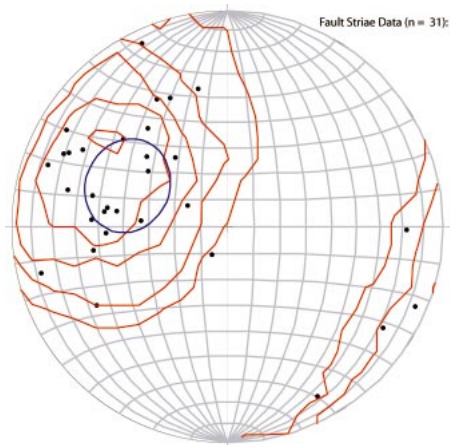

Figure 2. Scatter plot of fault striae for the Manly Pass fault zone in the northern part of the Slate Range. Mean vector plunges 48° toward 292°. Red lines are Kamb 2% contours (maximum = 10%). Blue oval is 95% confidence area for mean vector (radius is 17°).

as moderately consolidated alluvium. Slip on the Manly Pass fault is directed to the west-northwest (~290°; Fig. 2) as documented by slickenline measurements in the fault zone. We interpret the Manly Pass fault to be active despite a lack of young alluvial markers in the Slate Range. Our interpretation is based on several lines of evidence: (1) It is essentially continuous with the active trace of the Searles Valley fault, (2) It projects into active traces to the northeast across Panamint Valley (discussed below), and (3) Hanging wall faults within the range are clearly active based on earthquake distributions and faults cutting alluvial fans (Smith et al., 1968; Andrew and Walker, 2002).

The Manly Pass fault zone curves toward the northeast as it crosses the Slate Range (Fig. 1). The northeastward projection of this fault zone intersects the Panamint Range front at Manly canyon (the canyon containing Manly Fall). The alluvial fan at Manly canyon is cut by fault scarps indicating both strike-slip and normal offsets (Figs. 1 and 3). The strike-slip strands are continuous with faults of the Panamint Valley fault zone studied by Zhang et al. (1990) in the southern part of the area. The normal strands trend northeast, displace alluvial fan surfaces on the northern side of the Manly canyon fan, and are exactly on strike with the Manly Pass fault (Figs. 1 and 3). The faults do not cut across, but apparently merge with the NNW-striking scarps of the Panamint Valley fault zone. The age of the fan surface is uncertain, but the degree of soil de-
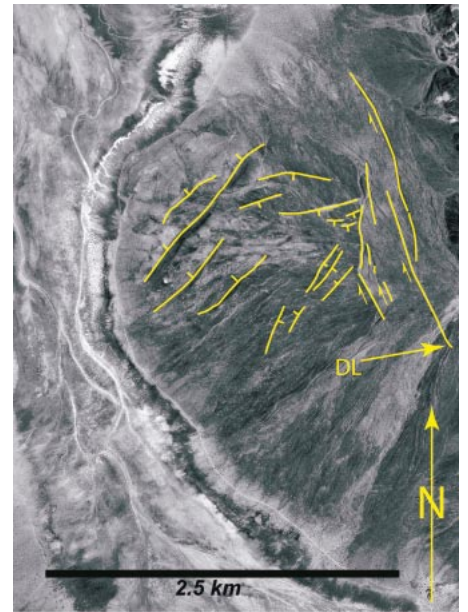

Figure 3. Orthophotograph of alluvial fan at the mouth of canyon below Manly Fall (here called Manly canyon). The NE-trending normal faults in the center of photo are the extension of the Manly Pass fault zone. These faults apparently terminate and merge to the east at the strike-slip faults of the Panamint Valley zone. Debris flow levees discussed in the text are at the southern end of a prominent strike-slip fault and location is shown with yellow line and arrow labeled with DL. Normal fault scarp noted in text is just off the photo to the right.

velopment, the presence of low shorelines near the modern playa, and the position of the fan relative to high shorelines along the range (e.g., Smith, 1976) all indicate that the Manly fan postdates the last occupation of high shorelines in the valley (likely ca. 120–150 ka; Jannik et al., 1991; Densmore and Anderson, 1997). Hence, faulting occurred within the last 120 ka, and very likely slip continued into the late Pleistocene.

Panamint Valley Fault Zone and the Ash Hill Fault

The Panamint Valley fault zone marks the western side of the Panamint Range (Fig. 1). Numerous fault scarps in young alluvium mark the trace of the fault zone for nearly 100 km along the range front (Zhang et al., 1990). Previous workers have presented conflicting interpretations for the kinematics of the fault zone. Burchfiel et al. (1987) suggested that the northern Panamint Valley developed because

of Pliocene-Recent displacement on a low-angle normal fault from a piercing point across the Hunter Mountain fault zone (a mostly strike-slip structure bounding the northern end of Panamint Valley and located ~45 km north of the area show in Fig. 1). Seismic and magnetic investigations in the northern part of the valley confirm that the sedimentary fill is thin (<200–300 m) and that basalts present in the hanging wall block are not buried beneath the valley (Biehler and the Massachusetts Institute of Technology Field Camp, 1987); both observations are consistent with oblique-normal displacement toward ~300° (parallel to the strike of the Hunter Mountain fault). In contrast, Zhang et al. (1990) presented observations from displaced geomorphic markers in the southern part of the valley that indicate a more northerly slip vector of ~340° (parallel to the strike of the Panamint Valley fault zone). They suggested a recent change in sense of slip was responsible for the significant right-lateral strike-slip observed along fault scarps south of Manly canyon (Fig. 1). Our study of the Panamint Valley fault zone leads us to a reinterpretation of the slip direction on the southern segment. We present these results in some detail in order to better define the net displacement direction for this segment of the fault zone.

South of Manly canyon, the Panamint Valley fault zone is marked by a prominent linear scarp trending ~340°. The scarp cuts all but the youngest alluvial fan surfaces in this portion of the valley. Just southwest of the head of the Manly canyon fan, the Panamint Valley fault zone consists of two distinct faults: a strike-slip fault and a normal fault, both of which offset the same debris-flow channel. The strike-slip fault displaces this channel in a right-lateral sense (Smith, 1976; Zhang et al., 1990). Although the age of this feature is unknown, the well-preserved character of the levees and minimal desert pavement within the abandoned channel suggest that it is late Pleistocene to Holocene in age (ca. <15–30 ka). There is some degree of uncertainty in the magnitude of displacement, however; Smith (1976) suggested an offset of ~20 m, while Zhang et al. (1990) indicated that the offset is as great as 27 m. In addition, neither study examined the prominent normal-sense fault scarp ~300 m to the east.

We surveyed the displaced levees of the debris flow with a survey-grade differential GPS to construct a high-resolution topographic map of the site. In addition, we used a laser range finder (3–5 cm precision) to survey displacements along the trace of the scarp. Both methods yielded consistent estimates of dis-
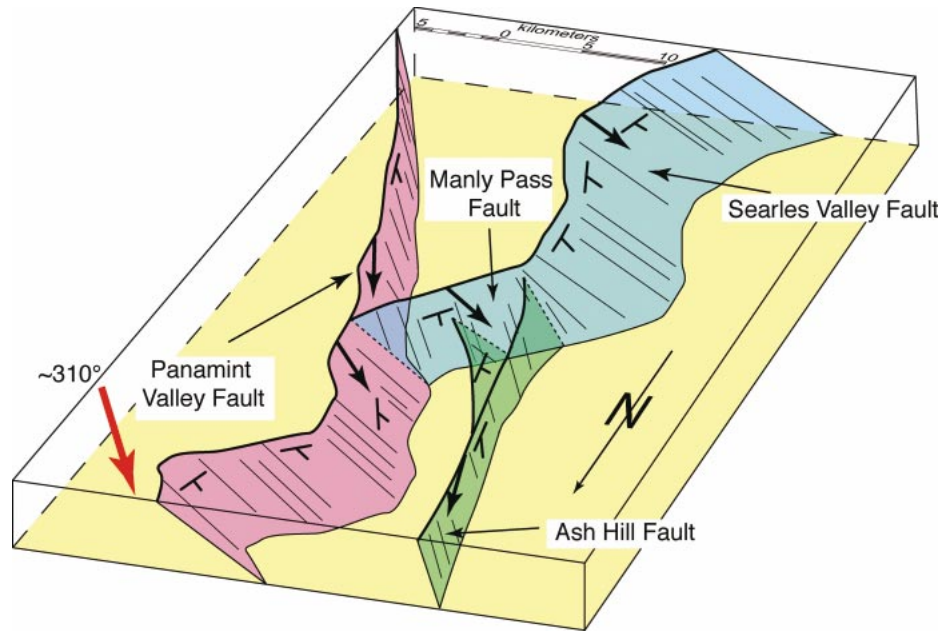

Figure 4. Block diagram showing the interaction of the Searles Valley, Manly Pass, Panamint Valley, and Ash Hill fault systems. Note that north is toward the lower left. The Ash Hill fault transfers to a complex array of faults that end at the Manly Pass fault (details of transfer are not shown here). Bold lines with arrows are the slip vectors for each segment of the fault system. Bold red arrow in lower left shows regional extension direction. Strike and dip symbols show local orientation of the fault zones. Figure inspired by diagram in Caskey et al. (1996).

placement; the northernmost levee has been offset by ~14 m while the southern levee has apparently been offset by ~19 m. No vertical offsets are apparent in this area. These estimates are significantly lower than the work by Zhang et al. (1990), but are in the range of Smith's (1976) estimates. Whether the discrepancy in displacement between individual levees reflects a true difference in age is uncertain. We note, however, that a second debris-flow just north of this site is also apparently offset by ~15 m. Thus, we consider 15–20 m a reasonable estimate for lateral displacement on this strand of the Panamint Valley fault since the formation of these debris flow levees.

In order to determine the total displacement on the Panamint Valley fault zone, however, we must also account for normal slip on a prominent scarp at the head of the Manly canyon fan. The same debris-flow channel described above continues to the east, up the fan, where it is cut by a ~10-m-high fault scarp. There is no apparent lateral offset of the channel at this site; offset is entirely dip-slip. If we assume a dip of 60° for the fault, the total horizontal displacement is ~6 m. Because the fault cuts the same channel, we sum displacement vectors for both scarps to yield a total

slip vector of 17–21 m toward ~320°. This is more westerly than the vector of Zhang et al. (1990).

In contrast, north of the intersection of the Manly Pass and Panamint Valley fault zones, the displacement vector shifts to a more westerly orientation. The fault zone takes a right-step, forming a ~3–5 km embayment in the range, northward to Happy Canyon (Fig. 1). Recent NE-trending fault scarps in the embayment exhibit almost pure dip slip, as evidenced by the displaced margin of a ca. 600-yr-old debris flow. The age of this flow comes from a ^{14}C date on a log contained within the debris flow (A. Cherkinsky, 2003, personal commun.). In addition, fault mullions and slickenlines on the NW-trending range front plunge shallowly (<10°) toward the northwest (Kirby et al., 2004). Both kinematic markers are consistent with the partitioning of oblique normal slip in a direction toward ~300°, subparallel to the long-term displacement vector in the northern Panamint Valley (Burchfiel et al., 1987). These observations led us to suggest that differences in fault kinematics observed by Burchfiel et al. (1987) and Zhang et al. (1990) reflect along-strike changes in displacement on the Panamint Valley fault zone due to the intersection with the Manly
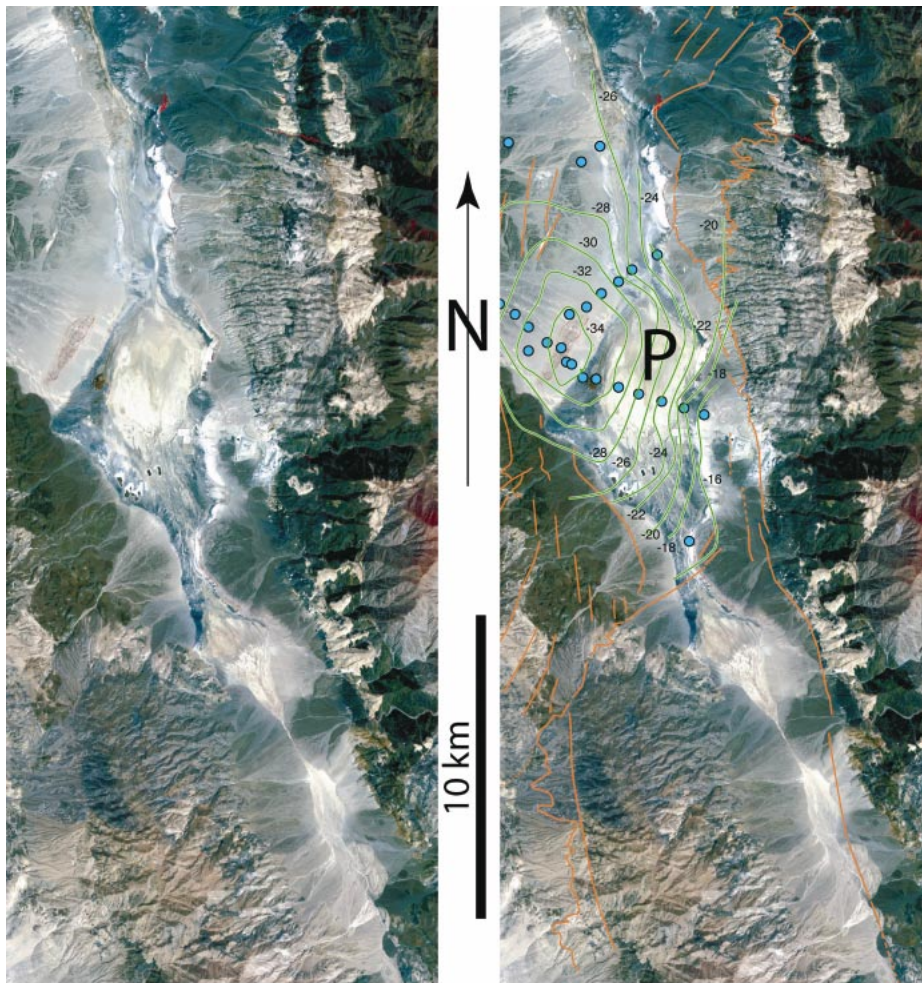
Figure 5. ASTER satellite image for the Panamint Valley and northern Slate Range. Left frame is the base image. Right frame overlain by faults shown on Figure 1. In addition, gravity contours (in mgal; green lines) are shown along with gravity observation points (blue points; data from Smith et al. [1968], and National Geophysical Data Center [1999]). P—prominent playa in southern Panamint Valley. Location shown on Figure 1.

Pass fault, rather than temporal changes in fault kinematics (see discussion below).

The last significant active structure in the region is the Ash Hill fault (Fig. 1). Densmore and Anderson (1997) presented a detailed study of the northern part of this fault and concluded that the fault is a slightly oblique, dextral strike-slip fault. Recent motion has a strike-slip to dip-slip ratio of 3.5:1, and net slip directed toward 320° to 330° (Densmore and Anderson, 1997, p. 57). This is significantly more northerly than the northern Panamint Valley fault zone. The Ash Hill fault continues southward into the northern Slate Range where it is part of the hanging wall of the Manly Pass zone. Fault geometry at the southern end consists of a complex zone of normal and strike-slip faults that vary in orientation from north-northwest to northeast

(Fig. 1). The reason for this complexity is uncertain, but it probably is related to the intersection of the Ash Hill with the Manly Pass fault. In this area, there apparently is a transition from primarily normal slip on the Manly Pass to mostly strike slip on the Ash Hill. The complex zone of faulting results from the merging of these systems. This system has been active in the last 120 k.y. (Densmore and Anderson, 1997), and the fresh nature of the youngest fault scarps suggests possible Holocene activity.

IMPLICATIONS FOR REGIONAL DEFORMATION

The fault zones described above have been active over the last 120–10 k.y. For this reason, and because of the fault interactions de-

scribed above and discussed below, we treat these structures as an integrated transtensional zone. We refer to areas north of the latitude of Manly canyon as the northern part of the system, and those to the south as the southern part. Based on geodetic (Unruh et al., 2002; Dixon et al., 2000) and geologic constraints (Wernicke and Snow, 1998; Snow and Wernicke, 2000), the maximum extension direction in the region is inferred to be toward ~310°. The summed slip on the faults described here should resolve to about this direction, although they clearly partition slip into different directions on each fault zone.

In Figure 4, we show a block diagram for our interpretation of fault interactions. A major assumption in this diagram is that the Manly Pass fault merges smoothly with the Panamint Valley fault. In addition, we consider the Panamint Valley fault zone to be formed by coordinated strike-slip and normal faults (e.g., as at Manly fan) moving on an overall low- to moderate-angle surface. This interpretation seems most consistent with the field relations we have observed (e.g., Andrew, 2002). This is at odds with the interpretations of Cichanski (2000), who considered the Panamint Valley fault a high-angle fault zone that cuts an older, low-angle normal fault system on the western flank of the Panamint Range. We also show the Ash Hill fault merging into the faulted hanging wall of the Manly Pass fault. Densmore and Anderson (1997) reported that the fault continues into this area and that complex faulting in Panamint Valley north of the Slate Range was also related to the Ash Hill fault. We do not show a relation between the Ash Hill and Panamint Valley fault, but consider it likely that the Ash Hill is a hanging wall splay of the Panamint Valley fault, a relation proposed by Densmore and Anderson (1997). The Manly Pass fault is contained in the hanging wall of the Panamint Valley fault, and the Ash Hill is confined to the hanging wall of the Manly Pass; for this reason, it seems simplest to interpret the Ash Hill fault to be confined to the hanging wall of the Panamint Valley fault.

Regional Strain Partitioning

Strain appears to be partitioned at the scale of the entire fault system. In the southern region, transtension is accommodated by primarily W-directed normal slip on the Searles Valley fault zone and by primarily strike-slip displacement on the southern Panamint Valley fault zone to the east (Fig. 4). To the north, however, active slip is partitioned into primarily strike-slip on the Ash Hill fault to the

west and into normal oblique slip on the Panamint Valley fault to the east. Although the magnitude of recent slip vectors is not well known and awaits a more complete chronology of alluvial deposits, the orientation of maximum extension across both the northern and southern portions of the fault system should yield similar directions.

Strain Transfer

The northern and southern segments of the fault systems are relatively simple in that displacement is localized primarily on two main faults. Complex fault geometries and strain transfers occur where the northern and southern segments meet in the northern Slate Range and Panamint Valley (Fig. 1 and 4). We discuss below mostly how strain transfers between the Manly Pass and Panamint Valley fault zones.

We noted above that the Manly Pass fault projects northeastward to prominent fault scarps on the alluvial fan at Manly canyon, and that these faults apparently merge there with the Panamint Valley fault zone. Several other important features are present. First, there is a pronounced negative gravity anomaly (Smith et al., 1968) in the southern Panamint Valley just north of the Manly canyon area (Fig. 5). This ~18-mgal anomaly is the largest in Panamint Valley, reflecting more than a kilometer of basin fill (assuming a density contrast of 0.35 g/cm³ between bedrock and basin fill—see also Jachens and Moring, 1990). No other comparable features are present elsewhere in Panamint Valley. Second, playa position and alluvial fan size are different along the Panamint Valley zone to the north and south of where the Manly Pass fault joins it. Alluvial fans are moderately to well developed to the south of Manly canyon and the active playa and/or drainages are roughly in the center of the valley; to the north, alluvial fans are very small, and the active playa is against the Panamint range front (Fig. 5).

We interpret this to indicate that subsidence is somewhat higher to the north of Manly fan because normal slip from the Manly Pass fault is added into the Panamint Valley fault zone. Both the gravity anomaly and the fan and/or playa positions are consistent with enhanced subsidence and normal-sense fault slip where the Manly Pass fault passes into the Panamint Valley zone. This interpretation fits well with the work of Maerten et al. (1999). These authors described slip on intersecting normal faults in modeling and field-based studies, and noted that areas of enhanced slip are expected for the block in the mutual hanging wall of
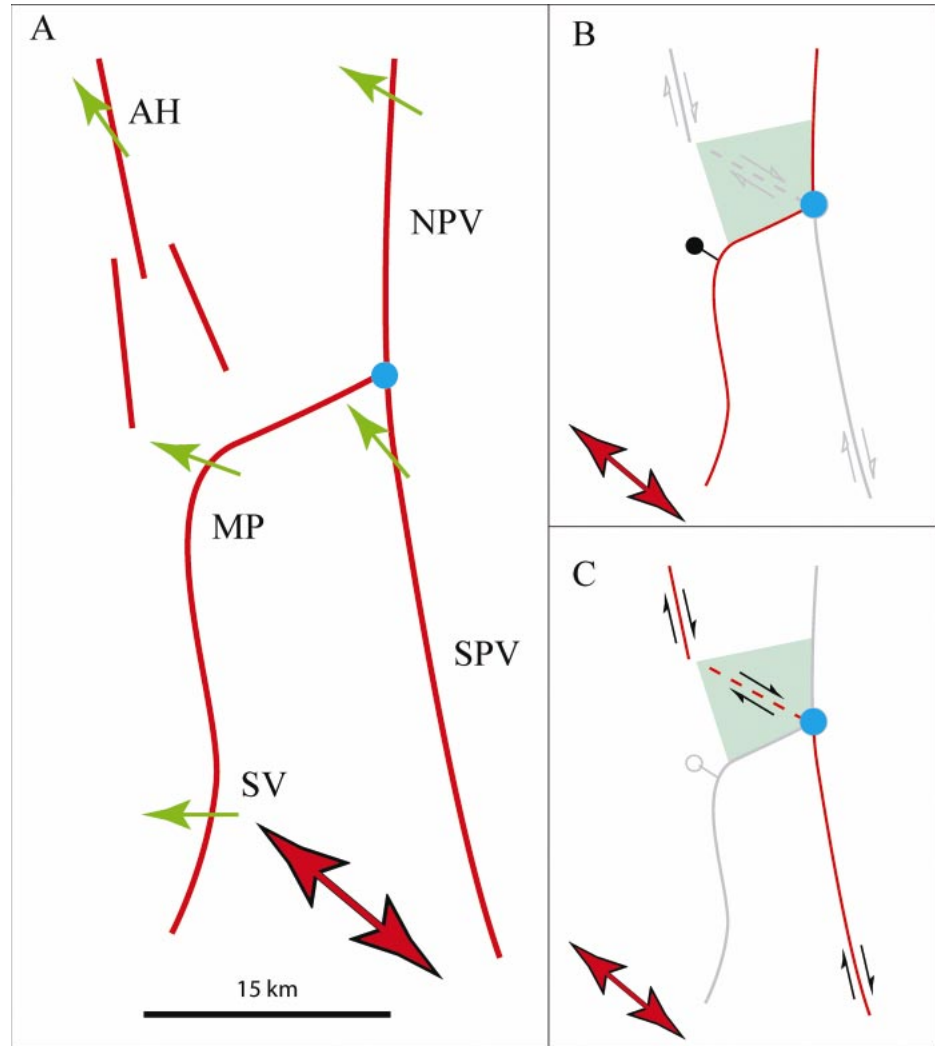

Figure 6. Schematic diagrams showing slip directions and fault interactions for the Searles Valley, Manly Pass, Panamint Valley, and Ash Hill fault zones. A: Main faults in system showing slip direction (green arrows) and regional maximum extension direction (red arrow). Blue dot shows the intersection point of the Manly Pass with the Panamint Valley fault zone. Same position is shown in other panels (along with regional direction) for reference. B: Diagram isolating the main normal faults in the system. The Manly Pass and northern Panamint Valley zones form a segmented normal fault. These faults are not perpendicular to extension direction, so some dextral shear must be accommodated by oblique slip and regional strike-slip faults (in gray color). Green triangular region shows area of highest subsidence inferred from slip on intersecting normal faults and proposed relay zone in strike-slip system (see below). C: Diagram isolating the mainly strike-slip faults in the system. The Ash Hill and southern Panamint Valley faults form a left-stepping geometry in the dextral system. Because deformation is transtensional, we hypothesize that the interactions of these faults occur on a connecting zone (schematically shown as dashed strike-slip fault) that is roughly parallel to the extension direction. No single fault connects these structures. See text for discussion of linkage.

the joining faults. Although the Maerten et al. (1999) study addressed the intersection of faults that tip out along strike, the results should still be generally applicable to the Panamint-Searles system of fully developed faults in a transtensional setting.

Transfer of westerly directed slip on the Manly Pass zone onto the Panamint Valley zone also causes the net slip direction to rotate about ~20° more westerly on the Panamint Valley zone, and the Panamint Valley zone changes from one that is mostly strike-slip to

the south to one that is dominantly normal to the north. This interaction appears to have been active over the last 10–~100 k.y. based on the ages of fans that are deformed by the faulting, and the presence of a deep basin where the faults interact suggests activity that is somewhat longer lived.

Strain transfer is complex for the Ash Hill to Manly Pass zone. The Ash Hill is a single fault trace in the northern part of Panamint Valley, but merges into a complex fault array southward to the hanging wall of the Manly Pass fault. Deformation in the hanging wall of the Manly Pass zone is directed to the northwest, rotated northward from that on the Manly Pass–Searles Valley system. The cause for this rotation must be the addition of slip from the Ash Hill fault.

We summarize the regional pattern of faults and slip directions in map view in Figure 6. The Panamint Valley zone can be divided into northern and southern segments with a change in slip direction occurring at the intersection with the Manly Pass fault (Fig. 6A). At a large scale, the Manly Pass and northern Panamint Valley zones constitute a single segmented normal fault (Fig. 6B). However, fault slip is at an angle to the regional extension direction. Some of the obliquity is accommodated by oblique slip on the fault segments, but much is apparently taken up on the strike-slip faults in the system. The strike-slip faults can also be viewed as a single dextral fault system; these faults have a left step-over geometry in the right-lateral system (Fig. 6C). Normally this should lead to restraining and/or contractional geometry; however, because the system is transtensional, the step-over can occur without net shortening (Fig. 6C).

This slip system implies two important conclusions: (1) The most complex pattern of faulting should occur in the area where the Ash Hill, Manly Pass, and Panamint Valley zones interact (e.g., in the area of the northern Slate Range and southern Panamint Valley). This is consistent with the position and complexity of active faults (Fig. 1). This interpretation was also made by Densmore and Anderson (1997) for the interaction of the Ash Hill with the Panamint Valley zone, and (2) The area of maximum basin subsidence should be in the same region. This owes to the effects of the intersecting normal faults (discussed above) and the transtensional step over from the Panamint Valley to the Ash Hill fault (Fig. 6C), and it is consistent with the gravity data and position of modern playas (Fig. 5).

CONCLUSIONS

Geologic mapping and displacement directions inferred from alluvial deposits along the Panamint Valley, Searles Valley, and Ash Hill fault systems yield new insight into the nature of fault interactions and strain transfer within active regions of transtensional deformation. In contrast to simple models for extensional links between subjacent strike-slip faults, our data suggest a complex, yet apparently stable array of interacting faults. The W-directed normal slip on the range-bounding Searles Valley fault zone is transferred across the Slate Range to feed into range-bounding slip on the Panamint Valley zone. At the intersection of these faults, slip on the Panamint Valley fault changes from primarily strike-slip, with minor extension, to the normal-oblique displacement that was responsible for the formation of present-day Panamint Valley. These geometries apparently have persisted for time scales $>10^5$ yr, and represent a quasi-stable system.

ACKNOWLEDGMENTS

REFERENCES CITED

Andrew, J.E., 2002, The Mesozoic and Tertiary tectonic history of the Panamint Range and Quail Mountains, California [Ph.D. thesis]: Lawrence, Kansas, University of Kansas, p. 154.

Andrew, J.E., and Walker, J.D., 2002, Geometry and kinematics of Miocene to Pleistocene transtension in the northern Slate Range, California: Geological Society of America Annual Meeting Abstracts with Programs, v. 34, no. 6, p. 178.

Bellier, O., and Zoback, M.L., 1995, Recent state of stress change in the Walker Lane zone, western Basin and Range province, United States: Tectonics, v. 14, p. 564–593, doi: 10.1029/94TC00596.

Benson, L.V., Currey, D.R., Dorn, R.I., Lajoie, K.R., Oviatt, C.G., Robinson, S.W., Smith, G.I., and Stine, S., 1990, Chronology of expansion and contraction of four Great Basin lake systems during the past 35,000 years: Palaeogeography, Palaeoclimatology, Palaeoecology, v. 78, p. 241–286, doi: 10.1016/0031-0182(90)90217-U.

Biehler, S., and the Massachusetts Institute of Technology Field Camp, 1987, A geophysical investigation of northern Panamint Valley, Inyo County, California: Journal of Geophysical Research, v. 92, p. 10,427–10,441.

Burchfiel, B.C., and Stewart, J.H., 1966, "Pull-apart" origin of the central segment of Death Valley, California: Geological Society of America Bulletin, v. 77, p. 439–442.

Burchfiel, B.C., Hodges, K.V., and Royden, L.H., 1987, Geology of Panamint Valley—Saline Valley pull-apart system, California: Palinspastic evidence for low-angle geometry of a Neogene range-bounding fault: Journal of Geophysical Research, v. 92, p. 10,422–10,426.

Caskey, S.J., Wesnousky, S.G., Zhang, P., and Slemmons, D.B., 1996, Surface faulting of the 1954 Fairview Peak (Ms 7.2) and Dixie Valley (Ms 6.8) earthquakes, central Nevada: Seismological Society of America Bulletin, v. 86, p. 761–787.

Cichanski, M., 2000, Low-angle, range-flank faults in Panamint, Inyo, and Slate ranges, California: Implications for recent tectonics of the Death Valley region: Geological Society of America Bulletin, v. 112, p. 871–883, doi: 10.1130/0016-7606(2000)112<0871:LARFFI>2.3.CO;2.

Cowie, P.A., and Scholz, C.H., 1992, Growth of faults by accumulation of seismic slip: Journal of Geophysical Research, v. 97, p. 11,085–11,095.

Dawers, N.H., Anders, M.H., and Scholz, C.H., 1993, Growth of normal faults: Displacement-length scaling: Geology, v. 21, p. 1107–1110, doi: 10.1130/0091-7613(1993)021<1107:GONFDL>2.3.CO;2.

Densmore, A.L., and Anderson, R.S., 1997, Tectonic geomorphology of the Ash Hill fault, Panamint Valley, California: Basin Research, v. 9, p. 53–63, doi: 10.1046/j.1365-2117.1997.00028.x.

Dewey, J.F., Holdsworth, R.E., and Strachan, R.A., 1998, Transpression and transtension zone, in Holdsworth, R.E., Strachan, R.A., and Dewey, J.F., eds., Continental transpressional and transtensional tectonics: Geological Society [London] Special Publication 135, p. 1–14.

Dixon, T.H., Miller, M., Farina, F., Wang, H., and Johnson, D., 2000, Present-day motion of the Sierra Nevada block and some tectonic implications for the Basin and Range province: North America Cordillera: Tectonics, v. 19, p. 1–24.

Dixon, T.H., Robaudo, J.L., and Reheis, M.C., 1995, Constraints on the present-day Basin and Range deformation from space geodesy: Tectonics, v. 14, p. 755–772, doi: 10.1029/95TC00931.

Faulds, J.E., and Varga, R.J., 1998, The role of accommodation zones and transfer zones in the regional segmentation of extended terranes: Geological Society of America Special Paper 323, p. 1–45.

Jachens, R.C., and Moring, B.C., 1990, Maps of the thickness of Cenozoic deposits and the isostatic residual gravity over basement for Nevada: U.S. Geological Survey Open-File Report 90–404, 15 p.

Jannik, N.O., Phillips, F.M., Smith, G.I., and Elmore, D., 1991, A ^{36}Cl chronology of lacustrine sedimentation in the Pleistocene Owens River system: Geological Society of America Bulletin, v. 103, p. 1146–1159, doi: 10.1130/0016-7606(1991)103<1146:ACCOLS>2.3.CO;2.

Kirby, E., Walker, J.D., Gosse, J., and McDonald, E., 2004, Late Quaternary–Recent slip on a low-angle normal fault: Inferences from alluvial deposits along the Panamint Valley fault system: Geological Society of America with Programs, v. 36, no. 5, p. 547.

Klinger, R.E., and Piety, L.A. 2001, Holocene faulting and slip rates along the Black Mountains fault zone near Mormon Point, in Machette, M.N., Johnson, M.L., and Slate, J.L., eds., Quaternary and late Pliocene geology of the Death Valley region; recent observations on tectonics, stratigraphy, and lake cycles: U.S. Geological Survey Open-File Report, p. L193–L203.

Lin, J.C., Broecker, W.S., Hemming, S.R., Hajdas, I., Anderson, R.F., Smith, G.I., Kelley, M., and Bonani, G., 1998, A reassessment of U-Th and ^{14}C ages for late-glacial high-frequency hydrologic events at Searles Lake, California: Quaternary Research, v. 49, p. 11–23, doi: 10.1006/qres.1997.1949.

Maerten, L., Willemse, E.J.M., Pollard, D.D., and Rawnsley, K.D., 1999, Slip distribution on intersecting normal faults: Journal of Structural Geology, v. 21, p. 259–271, doi: 10.1016/S0191-8141(98)00122-9.

Manighetti, I., Tapponnier, P., Courtillot, V., Gallet, Y., Jacques, E., and Gillot, P.-Y., 2001, Strain transfer between disconnected, propagating rifts in Afar: Journal of Geophysical Research, v. 106, p. 13,613–13,665, doi: 10.1029/2000JB900454.

McClusky, S.C., Bjornstad, S.C., Hager, B.H., King, R.W.,

Meade, B.J., Miller, M.M., Monastero, F.C., and Souter, B.J., 2001, Present day kinematics of the Eastern California Shear Zone from a geodetically constrained block mode: Geophysical Research Letters, v. 28, p. 3369–3372, doi: 10.1029/2001GL013091.

Miller, M., Johnson, D.J., Dixon, T.H., and Dokka, R.K., 2001, Refined kinematics of the Eastern California shear zone from GPS observations, 1993–1998: Journal of Geophysical Research, v. 106, p. 2245–2263, doi: 10.1029/2000JB900328.

Monastero, F.C., Walker, J.D., Katzenstein, A.M., and Sabin, A.E., 2002, Neogene evolution of the Indian Wells Valley, east-central California, *in* Glazner, A.F., Walker, J.D., and Bartley, J.M., eds., Geologic evolution of the Mojave Desert and Southwestern Basin and Range: Geological Society of America Memoir 195, p. 199–228.

Moore, S.C., 1976, Geology and thrust fault tectonics of parts of the Argus and Slate ranges, Inyo County, California [Ph.D. thesis]: Seattle, Washington, University of Washington, 127 p.

National Geophysical Data Center, 1999, Land and marine gravity CD-ROMs, Compiled by David Dater, Dan Metzger, and Allen Hittelman: Boulder, Colorado, U.S. Department of Commerce, National Oceanic and Atmospheric Administration, National Geophysical Data Center.

Numelin, T., and Kirby, E., 2004, Evidence for Quaternary slip on a low angle normal fault: Searles Valley, California: EOS (Transactions, American Geophysical Union), v. 85, no. 47.

Oldow, J.S., 1992, Late Cenozoic displacement partitioning in the northwestern Great Basin, *in* Craig, S.D., ed., Walker Lane symposium; structure, tectonics & min-eralization of the Walker Lane: Reno, Nevada, Geological Society of Nevada, p. 17–52.

Reheis, M.C., and Dixon, T.H., 1996, Kinematics of the eastern California shear zone; evidence for slip transfer from Owens and Saline Valley fault zones to Fish Lake Valley fault zone: Geology, v. 24, p. 339–342, doi: 10.1130/0091-7613(1996)024<0339:KOTECS>2.3.CO;2.

Smith, G.I., Troxel, B.W., Gray, C.H., and von Huene, R., 1968, Geologic reconnaissance of the Slate Range, San Bernardino and Inyo counties, California: California Division of Mines and Geology Special Report 96, 33 p.

Smith, G.I., and Street-Perrott, F.A., 1984, Pluvial lakes of the western United States, *in* Porter, S.C., ed., The late Pleistocene (late Quaternary environments of the United States): Minneapolis, University of Minnesota Press, p. 190–212.

Smith, R.S.U., 1976, Late-Quaternary fluvial and tectonic history of Panamint Valley, Inyo and San Bernardino counties, California [Ph.D. thesis]: Pasadena, California, California Institute of Technology, 314 p.

Snow, J.K., and Wernicke, B.P., 2000, Cenozoic tectonism in the central Basin and Range: Magnitude, rate, and distribution of upper crustal strain: American Journal of Science, v. 300, no. 9, p. 659–719.

Unruh, J.R., Hauksson, E., Monastero, F.C., Twiss, R.J., and Lewis, J.L., 2002, Seismotectonics of the Coso Range-Indian Wells Valley region, California: Transtensional deformation along the southeastern margin of the Sierran microplate, *in* Glazner, A.F., Walker, J.D., and Bartley, J.M., eds., Geological evolution of the Mojave Desert and southwestern Basin and Range: Geological Society of America Memoir 195, p. 277–294.

Walker, J.D., Berry, A.K., Davis, P.J., Andrew, J.E., and Mitsdarfer, J.M., 2002, Geologic compilation map of the northern Mojave Desert and southwestern Basin and Range province, *in* Glazner, A.F., Walker, J.D., and Bartley, J.M., eds., Geologic evolution of the Mojave Desert and southwestern Basin and Range: Geological Society of America Memoir 195, p. 297–299.

Wallace, R.E., 1984, Patterns and timing of late Quaternary faulting in the Great Basin province and relation to some regional tectonic features: Journal of Geophysical Research, v. 89, p. 5763–5769.

Wernicke, B., Axen, G.J., and Snow, J.K., 1988, Basin and Range extensional tectonics at the latitude of Las Vegas, Nevada: Geological Society of America Bulletin, v. 100, p. 1738–1757, doi: 10.1130/0016-7606(1988)100<1738:BARETA>2.3.CO;2.

Wernicke, B., and Snow, J.K., 1998, Cenozoic tectonism in the central Basin and Range: Motion of the Sierra-Great Valley block, *in* Ernst, W.G., and Nelson, C.A., eds., Integrated Earth and environmental evolution of the Southwestern United States: Columbia, Bellwether Publishing, p. 111–118.

Zhang, P., Ellis, M., Slemmons, D.B., and Mao, F., 1990, Right-lateral displacements and the Holocene slip rate associated with prehistoric earthquakes along the southern Panamint Valley fault zone; implications for southern Basin and Range tectonics and coastal California deformation: Journal of Geophysical Research, v. 95, p. 4857–4872.